Final state interactions in ^{4}He(e,e'p)^{3}H at large proton energy

O. Benhar [a] N.N. Nikolaev [b,c] J. Speth [b] A.A. Usmani [d]
B.G. Zakharov [c]

[a]*INFN, Sezione Roma 1, I-00185 Rome, Italy*

[b]*IKP(Theorie), Forschungszentrum Jülich GmbH. D-52425 Jülich, Germany*

[c]*L.D.Landau Institute for Theoretical Physics,
117940, ul. Kosygina 2, V-334 Moscow, Russia*

[d]*Physics Department, Aligarh Muslim University, Aligarh-202 002, India*

Abstract

At large proton energy, the final state interactions of the knocked out nucleon in $(e, e'p)$ reactions off nuclear targets can be described within the eikonal approximation, treating the spectator particles as a collection of fixed scattering centers. We use a generalization of this approach, suitable to take into account the possible occurrence of color transparency, to carry out an accurate calculation of the missing momentum distribution of the process $^4He(e, e'p)^3H$. The pattern of final state interaction effect is analyzed for different kinematical setups in the domain corresponding to $2 \leq Q^2 \leq 20$ (GeV/c)^2.

Key words: Electron-nucleus scattering. Final state interactions. Few nucleon systems.

1 Introduction

Electron-nucleus scattering experiments in which a proton is detected in coincidence with the outgoing electron have long been recognized as a powerful tool to study both nuclear and nucleon dynamics (see, e.g., ref.[1]). According to the Plane Wave Impulse Approximation (PWIA), which is expected to be valid at large momentum transfer, the nuclear $(e, e'p)$ cross section reduces to the incoherent sum of the cross sections off individual nucleons, whose distribution in momentum **k** and removal energy E is dictated by the spectral function $P(k, E)$, the final state interactions (FSI) between the knocked out

particle and the recoiling spectator system being negligible. As a consequence, the PWIA cross section of the process in which an electron of initial energy E_i is scattered into the solid angle Ω_e with energy $E_f = E_i - \omega$, while a proton of kinetic energy T_p is ejected into the solid angle Ω_p, takes the simple factorized form

$$\frac{d\sigma}{d\omega d\Omega_e d\Omega_p dT_p} = p(T_p + m)\tilde{\sigma}_{ep}P(p_m, E_m) , \tag{1}$$

where m denotes the nucleon mass, while the missing momentum $\mathbf{p}_m$ and missing energy E_m are defined as

$$\mathbf{p}_m = \mathbf{p} - \mathbf{q} \tag{2}$$

and

$$E_m = \omega - T_p - T_R . \tag{3}$$

In the above equations, $\mathbf{q}$ is the momentum transfer and $T_R = p_R^2/M_{A-1}$, with $\mathbf{p}_R = -\mathbf{p}_m$, is the kinetic energy of the recoiling spectator system of mass M_{A-1}. The cross section $\tilde{\sigma}_{ep}$ of eq.(1) describes electron scattering off a *bound* nucleon of momentum $\mathbf{p}_m$ and removal energy E_m [2].

In presence of nonnegligible FSI, the PWIA picture breaks down, and the missing momentum and energy cannot be readily interpreted as the initial momentum and removal energy of the outgoing nucleon. Therefore, a quantitative understanding of FSI is needed in order to extract the information on the nucleon spectral function from the measured $(e, e'p)$ cross section. A wealth of highly accurate theoretical calculations of FSI effects in $(e, e'p)$ reactions have been carried out within the Distorted Wave Impulse Approximation (DWIA), in which the interaction between the knocked out nucleon and the spectator system is described in terms of a complex optical potential (see, e.g., ref.[3]). Using the results of these calculations it has been possible to obtain the spectral functions describing the single-particle states, predicted by the nuclear shell model, from the analysis of the available low missing energy data [4].

It has to be emphasized, however, that FSI should not only be regarded as a *noise*, to be removed from the measured cross sections. In fact, in many instances FSI produce a *signal* that carries relevant information on both the target structure and the dynamics of the scattering process. For example, it has been shown that FSI effets, which obviously depend upon the distribution in space of the spectator particles, are very sensitive to the presence of local fluctuations of the nuclear density produced by nucleon-nucleon (NN) correlations [5].

The analysis of FSI in $(e, e'p)$ processes may also provide information on NN scattering in the nuclear medium. At moderate proton energies (~ 100 MeV) *nuclear* structure effects, such as Pauli blocking and dispersive corrections, lead to significant changes in the NN scattering amplitude [6]. While these effects are expected to become negligible for proton energies in the few GeV range, different effects, arising from *nucleon* structure, may become important in this kinematical regime, corresponding to high Q^2 ($Q^2 = q^2 - \omega^2$).

Perturbative Quantum Chromo-Dynamics (QCD) predicts that elastic scattering on a nucleon at high momentum transfer can only occur if the nucleon is found in the Fock state having the lowest number of constituents, so that the momentum can be most effectively shared among them. This state, being very compact, interacts weakly with the spectator particles and evolves to the standard proton configuration with a characteristic timescale that increases with the momentum transfer. According to this picture a proton, after absorbing a large momentum q, e.g. in an electron scattering process, can travel through the spectator system experiencing very little attenuation, i.e. exhibits *color transparency* (CT) [7,8]. In the limit $Q^2 \to \infty$ FSI effects in $(e, e'p)$ are expected to become vanishingly small.

The possible signatures of the occurrence of CT in coincidence $(e, e'p)$ and $(p, 2p)$ processes have been recently studied within a theoretical many-body approach suitable for the calculation of semi-inclusive cross sections, involving a sum over the states of the undetected spectator system [9–11]. The treatment of FSI of refs.[9–11] is based on a generalization of Glauber theory of high energy proton scattering [12].

In this paper we extend the approach of refs.[9–11] to the case of fully exclusive reactions, in which the final state of the recoiling nucleus is specified. Our treatment of the corresponding amplitude is presented in section II, where we discuss both the many-body aspects, related to the description of the nuclear initial and final states, and the structure of the scattering operator, modeling the FSI of the knocked out proton and the transition to the CT regime. The results obtained applying our approach to the case of a ^{4}He target, in which accurate numerical calculations are feasible, are given in section III, where FSI effects on different observables are discussed. Finally, the summary and conclusions are presented in section IV.

2   Formalism

2.1 $(e, e'p)$ *amplitude at high proton energy*

We will focus on $(e, e'p)$ processes in which the recoiling (A-1)-particle system is left in a bound state $|\varphi_n\rangle$. Neglecting many-body contributions to the electromagnetic current, the nuclear matrix element associated with the transition amplitude can be written

$$M_n(\mathbf{p}, \mathbf{q}) = \langle \Psi_{n\mathbf{p}}^{(-)}| \sum_{\mathbf{k}} a_{\mathbf{k}+\mathbf{q}}^{\dagger} a_{\mathbf{k}}|\Psi_0\rangle \ , \tag{4}$$

where $a_{\mathbf{k}+\mathbf{q}}^{\dagger}$ $(a_{\mathbf{k}})$ denotes the usual creation (anihilation) operator and the target ground state $|\Psi_0\rangle$ satisfies the Schrödinger equation $H_A|\Psi_0\rangle = E_0|\Psi_0\rangle$.

The terms responsible for FSI can be isolated in H_A rewriting the nuclear hamiltonian in the form

$$H_A = \sum_{i=1}^{A} T_i + \sum_{j>i=1}^{A} v_{ij} = H_0 + H_1 \ , \tag{5}$$

with (the knocked out nucleon is labelled with index 1)

$$H_0 = \sum_{i=1}^{A} T_i + \sum_{j>i=2}^{A} v_{ij} = H_{A-1} + T_1 \ , \tag{6}$$

and

$$H_1 = \sum_{j=2}^{A} v_{1j} \ . \tag{7}$$

In the above equations T_i and v_{ij} denote the kinetic energy of the i-th nucleon and the interaction potential between nucleons i and j, respectively. H_0 is the PWIA hamiltonian, describing the system containing (A-1) interacting spectators and the noninteracting knocked out nucleon, whereas the terms associated with FSI are included in H_1.

The decomposition of eq.(5) can be used to write the final scattering state $|\Psi_{n\mathbf{p}}^{(-)}\rangle$, in the form [13]:

$$|\Psi_{n\mathbf{p}}^{(-)}\rangle = \Omega_{\mathbf{p}}^{(-)}|\Phi_{n\mathbf{p}}\rangle \ , \tag{8}$$

where $|\Phi_{n\mathbf{p}}\rangle$ denotes the asymptotic state with no interaction between particle 1 and the spectators, which is obviously an eigenstate of H_0. In coordinate

space it can be written

$$\Phi_{n\mathbf{p}}(R) = \sqrt{\frac{1}{V}} \, e^{i\mathbf{p}\cdot\mathbf{r}_1} \varphi_n(\widetilde{R}) \, , \tag{9}$$

where V is the normalization volume, while $R \equiv \{\mathbf{r}_1, \mathbf{r}_2 \ldots, \mathbf{r}_A\}$ and $\widetilde{R} \equiv \{\mathbf{r}_2, \ldots, \mathbf{r}_A\}$ specify the configurations of the full A-particle system and the (A-1)-particle spectator system, respectively.

Setting $\Omega_{\mathbf{p}}^{(-)} = 1$, which amounts to disregarding the effects of FSI, and substituting into eq.(4), one obtains the PWIA amplitude, depending upon the the missing momentum $\mathbf{p}_m = \mathbf{p} - \mathbf{q}$ only. The operator $\Omega_{\mathbf{p}}^{(-)}$ describes the distortion of the asymptotyc wave function produced by the rescattering of the knocked out nucleon. It can be formally written as

$$\Omega_{\mathbf{p}}^{(-)} = \lim_{t\to\infty} e^{iH_A t} e^{-iH_0 t} = \lim_{t\to\infty} \widehat{T} e^{-i\int_0^t dt' \, \widehat{H}_1(t')} \, , \tag{10}$$

where $\widehat{T}$ denotes the time ordering operator and

$$\widehat{H}_1(t) = e^{iH_0 t} H_1 e^{-iH_0 t} \, . \tag{11}$$

In general, the calculation of $\Omega_{\mathbf{p}}^{(-)}$ from eq.(10) with a realistic nuclear hamiltonian involves prohibitive difficulties. However, when the kinetic energy carried by the knocked out proton is large, the structure of $\Omega_{\mathbf{p}}^{(-)}$ can be strongly simplified using a generalization of the approximation scheme originally developed by Glauber to decribe proton-nucleus scattering [12]. The basic assumptions underlying this scheme are that i) the fast struck nucleon moves along a straight trajectory, being undeflected by rescattering processes (*eikonal approximation*) and ii) the spectator system can be seen as a collection of fixed scattering centers (*frozen approximation*).

Implementation of the eikonal and frozen approximations in the definition of the scattering operator $\Omega_{\mathbf{p}}^{(-)}$, eq.(10), leads to the following coordinate space expression:

$$\Omega_{\mathbf{p}}^{(-)}(R) = \langle R|\Omega_{\mathbf{p}}^{(-)}|R\rangle = P_z \prod_{j=2}^{A} [1 - \Gamma_p(1,j)]$$

$$= P_z \left[1 - \sum_{j=2}^{A} \Gamma_p(1,j) + \sum_{k>j=2}^{A} \Gamma_p(1,j)\Gamma_p(1,k) - \ldots \right] \, , \tag{12}$$

where the positive z-axis is chosen along the eikonal trajectory and the z-ordering operator P_z prevents the occurrence of backward scattering of the

fast struck proton. The structure of the two-body operator $\Gamma_p(1, j)$, describing the dynamics of the scattering process, will be discussed in the next section.

Inserting $\Omega_{\mathbf{p}}^{(-)}$ of eq.(12) into the definition of $|\Psi_{n\mathbf{p}}^{(-)}\rangle$ of eq.(8) one gets the following expression for the matrix element of eq.(4):

$$M_n(\mathbf{p}, \mathbf{q}) = \int dR \left[\varphi_n(\widetilde{R}) \Omega_{\mathbf{p}}^{(-)}(R) \right]^* e^{i(\mathbf{p}-\mathbf{q})\cdot\mathbf{r}_1} \Psi_0(R) \ . \tag{13}$$

The calculation of the above amplitude can be simplified introducing a further approximation, whose validity rests on the same assumptions made to justify the use of the frozen approximation. Within this scheme [14], one replaces the many-body scattering operator $\Omega_{\mathbf{p}}^{(-)}(R)$ with a one-body operator, depending on the position of the knocked out nucleon only, that can be obtained averaging $\Omega_{\mathbf{p}}^{(-)}(R)$ over the positions of the spectator particles in the target ground state according to the following definition:

$$\overline{\Omega}_{\mathbf{p}}^{(-)}(\mathbf{r}) = \frac{1}{\rho_A(\mathbf{r})} \int dR \ |\Psi_0(R)|^2 \ \Omega_{\mathbf{p}}^{(-)}(R) \ \frac{1}{A} \sum_{i=1}^A \delta(\mathbf{r} - \mathbf{r}_i) \ , \tag{14}$$

where $\rho_A(\mathbf{r})$ is the target density normalized to unity.

Substitution of $\Omega_{\mathbf{p}}^{(-)}(R)$ with $\overline{\Omega}_{\mathbf{p}}^{(-)}(\mathbf{r})$ in eq.(13) allows one to rewrite the amplitude in the form:

$$M_n(\mathbf{p}, \mathbf{q}) = \int d^3r \ e^{i(\mathbf{p}-\mathbf{q})\cdot\mathbf{r}} \psi_{n\mathbf{p}}(\mathbf{r}) \ , \tag{15}$$

the *distorted overlap* $\psi_{n\mathbf{p}}(\mathbf{r})$ being defined as:

$$\psi_{n\mathbf{p}}(\mathbf{r}) = \left[\overline{\Omega}_{\mathbf{p}}^{(-)}(\mathbf{r}) \right]^* \chi_n(\mathbf{r}) \ , \tag{16}$$

with

$$\chi_n(\mathbf{r}_1) = \int d\widetilde{R} \ \varphi_n^*(\widetilde{R}) \Psi_0(R) \ . \tag{17}$$

Note that, within the nuclear shell model picture, the quantity defined in eq.(17) can be interpreted as the wave function associated with the single particle state initially occupied by the knocked out nucleon [15].

The overlap relevant to the case of proton knock out from a ^{4}He target leading to a recoiling ^{3}H can be written:

$$\chi_0(\mathbf{X}) = \int d^3Y d^3Z \ \Psi_3^*(\mathbf{Y}, \mathbf{Z}) \ \Psi_4(\mathbf{X}, \mathbf{Y}, \mathbf{Z}) \ , \tag{18}$$

with $\mathbf{Y} = \mathbf{r}_2 - \mathbf{r}_3$, $\mathbf{Z} = (2/3)\mathbf{r}_4 - (\mathbf{r}_2 + \mathbf{r}_3)/3$, $\mathbf{X} = \mathbf{r}_1 - (\mathbf{r}_2 + \mathbf{r}_3 + \mathbf{r}_4)/3$, whereas $\Psi_3(\mathbf{Y}, \mathbf{Z})$ and $\Psi_4(\mathbf{X}, \mathbf{Y}, \mathbf{Z})$ denote the ground state wave functions of ^{3}H and ^{4}He, respectively. The function $\chi_0(\mathbf{X})$ has been evaluated by Schiavilla et al with highly realistic wave functions, obtained using the Variational Monte Carlo approach and nuclear hamiltonians including two- and three-nucleon interactions [16]. We have used the results of ref.[16] to calculate the amplitude of eq.(15) with the averaged scattering operator given by eq.(14), whose definition in the ^{4}He center of mass frame reads

$$\overline{\Omega}_{\mathbf{p}}^{(-)}(\mathbf{X}) = \frac{\int d^3Y\, d^3Z \, |\Psi_4(\mathbf{X}, \mathbf{Y}, \mathbf{Z})|^2 \, \Omega_{\mathbf{p}}^{(-)}(\mathbf{X}, \mathbf{Y}, \mathbf{Z})}{\int d^3Y\, d^3Z \, |\Psi_4(\mathbf{X}, \mathbf{Y}, \mathbf{Z})|^2} \; . \tag{19}$$

The integrations involved in the calculation of $\overline{\Omega}_{\mathbf{p}}^{(-)}(\mathbf{X})$ have been carried out using Monte Carlo configurations sampled from the probability distribution associated with the ^{4}He ground state wave function of ref.[16].

2.2   Scattering operator

Within standard nonrelativistic nuclear many-body theory, i.e. treating the nucleons as pointlike structureless particles, the operator $\Gamma_p(1, j)$ appearing in eq.(12) is a function of the particle positions $\mathbf{r}_1$ and $\mathbf{r}_j$ only. Choosing the z axis along the direction of the eikonal trajectory (i.e. the direction of the momentum of the struck proton, specified by the unit vector $\mathbf{p}/|\mathbf{p}|$, the dependence of $\Gamma_p(1, j)$ upon z_1 and z_j can be singled out writing

$$\Gamma_p(1, j) = \theta(z_j - z_1)\gamma_p(|\mathbf{b}_1 - \mathbf{b}_j|) \; , \tag{20}$$

where the step function preserves causality while $\gamma_p(b)$ is a function of the projection of the interparticle distance in the impact parameter plane (the xy plane) which contains all the information on the dynamics of the scattering process. The function $\gamma_p(b)$ can be simply related to the coordinate space t-matrix associated with the proton-nucleon (pN) potential v_{ij}, and written in terms of the measured NN scattering amplitude at incident momentum p, $f_p(k_t)$, as

$$\gamma_p(b) = -\frac{i}{2} \int \frac{d^2k_t}{(2\pi)^2} \; e^{i\mathbf{k}_t \cdot \mathbf{b}} \; f_p(k_t) \; . \tag{21}$$

At large p, the experimental $f_p(k_t)$ is usually parametrized in the form [17]

$$f_p(k_t) = i \; \sigma_{pN}^{tot}(1 - i\alpha_{pN})e^{-\frac{1}{2}\frac{k_t^2}{B}} \; , \tag{22}$$

7

where σ_{pN}^{tot} and α_{pN} denote the total cross section and the ratio between the real and the imaginary part of the amplitude, respectively, while B is related to the range of the interaction. In the case of zero-range interaction, $B = 0$ and the impact parameter dependence of $\gamma_p(b)$ reduces to a two-dimensional δ-function.

To include CT, the internal structure of the proton must be explicitly taken into account. According to the CT scenario, in the $(e, e'p)$ reaction at large Q^2 the electromagnetic interaction produces a compact three-quark state $|E\rangle$, which can be seen as a superposition of many hadronic states $|\alpha\rangle, |\beta\rangle \dots$. This state then propagates through the nuclear medium undergoing rescattering processes that eventually lead to the emergence of the detected proton. The rescattering processes can be either *diagonal*, when the hadronic state $|\alpha\rangle$ does not change, or *off diagonal*, when a transition to a different state $|\beta\rangle$ is induced. The transparency effect, i.e. the disappearance of nuclear absorption, folows from the cancelation between the contributions of *diagonal* and *off diagonal* processes at asymptotically high Q^2.

From the above discussion , it follows that, in order to describe the transition of FSI effects to the CT regime, one has to introduce a scattering operator acting in the space of the hadronic states. Its matrix element between states $|\beta\rangle$ and $|\alpha\rangle$, of mass m_β and m_α, respectively, can be defined as [10]

$$\langle\beta|\Gamma_p(1,j)|\alpha\rangle = \theta(z_j - z_1)e^{ik_{\alpha\beta}z_j}\gamma_p^{\alpha\beta}(|\mathbf{b}_1 - \mathbf{b}_j|) , \tag{23}$$

where

$$k_{\alpha\beta} = \frac{m_\alpha^2 - m_\beta^2}{2E_p} , \tag{24}$$

$E_p = T_p + m$ being the energy of the detected proton in the laboratory frame. The onset oc CT is driven by the oscillating factors $\exp(ik_{\alpha\beta}z_j)$, taking into account the longitudinal momentum transfer associated with each transition $\alpha + N \rightarrow \beta + N$. In analogy to eq.(21), $\gamma_p^{\alpha\beta}(b)$ is written in terms of the amplitude of the process $\alpha + N \rightarrow \beta + N$:

$$\gamma_p^{\alpha\beta}(b) = -\frac{i}{2} \int \frac{d^2k_t}{(2\pi)^2} \, e^{i\mathbf{k}_t\cdot\mathbf{b}} \, f_p^{\alpha\beta}(k_t) , \tag{25}$$

with

$$f_p^{\alpha\beta}(k_t) = i \, \langle\beta|\hat{\sigma}|\alpha\rangle(1 - i\alpha_{\alpha\beta})e^{-\frac{1}{2}\frac{k_t^2}{B_{\alpha\beta}}} . \tag{26}$$

In the above equation, $\alpha_{\alpha\beta}$ and $B_{\alpha\beta}$ are the generalization of the parameters α_{pN} and B of eq.(22), while the operator $\hat{\sigma}$ describes the hadronic cross section. Unfortunately, $\alpha_{\alpha\beta}$ and $B_{\alpha\beta}$ are not known experimentally. In our numerical calculations we have made the assumption that the interactions responsible for off diagonal rescatterings have zero range, i.e. that $B_{\alpha\beta} = 0$ for any $\alpha \neq \beta$. The values of $\alpha_{\alpha\beta}$ have been varied within a reasonable range to gauge the sensitivity of our approach to these parameters. The results will be discussed in the next section.

Following ref.[9], $\langle\beta|\hat{\sigma}|\alpha\rangle$ has been evaluated in configuration space, using

$$\langle\beta|\hat{\sigma}|\alpha\rangle = \int d\xi d^2\rho \; \psi_\beta^*(\xi,\rho)\sigma(\rho)\psi_\alpha(\xi,\rho) \; , \tag{27}$$

where ψ_α and ψ_β are harmonic oscillator wave functions describing a quark-diquark system with longitudinal and transverse coordinates ξ and ρ, respectively. The quark-diquark oscillation frequency has been chosen to be $\omega_0 = 0.35$ GeV [9], yielding a realistic mass spectrum of the proton excited states, while $\sigma(\rho)$ has been parametrized in the form [18]

$$\sigma(\rho) = \sigma_0 \left[1 - e^{-\left(\frac{\rho}{\rho_0}\right)^2} \right] \; , \tag{28}$$

with $\sigma_0 = 2\sigma_{pN}$ and ρ_0 adjusted in such a way as to reproduce the experimental pN total cross section.

A scattering operator suitable to describe the onset of CT, denoted $\Omega_{CT}(R)$, can be constructed using eq.(12) and the two-body scattering operators $\Gamma_p(1,j)$ whose matrix elements are defined by eq.(23):

$$\begin{aligned}
\Omega_{\mathbf{p}}^{CT}(R) &= \frac{P_z\langle p| \prod_{j=2}^{A} [1 - \Gamma_p(1,j)] |E\rangle}{\langle p|E\rangle} \\
&= 1 - P_z \sum_{j=2}^{A} \sum_{\alpha} \langle p|\Gamma_p(1,j)|\alpha\rangle \frac{\langle\alpha|E\rangle}{\langle p|E\rangle} \\
&+ P_z \sum_{k>j=2}^{A} \sum_{\alpha\beta} \langle p|\Gamma_p(1,k)|\beta\rangle\langle\beta|\Gamma_p(1,j)|\alpha\rangle \frac{\langle\alpha|E\rangle}{\langle p|E\rangle} + \dots \; , \tag{29}
\end{aligned}$$

where $|p\rangle$ is the state describing the detected proton. For the compact state $|E\rangle$ produced at the electromagnetic vertex, we have used the same configuration space wave function employed in refs.[9,10]

$$\langle\rho|E\rangle \propto e^{-C\rho^2 Q^2} \; , \tag{30}$$

with $C = 1$. It has to be pointed out that, as shown in ref.[9], the missing momentum distribution is not sensitive to the choice of C as long as $C \geq 0.05$.

3   Results

Using the functions $\chi_0(\mathbf{X})$ and $\overline{\Omega}_{\mathbf{p}}^{(-)}(\mathbf{X})$ defined by eqs.(18) and (19), respectively, the missing momentum distribution associated with the $^4He(e, e'p)^3H$ process, denoted $W_{\mathbf{p}}(\mathbf{p}_m)$, can be readily obtained from

$$W_{\mathbf{p}}(\mathbf{p}_m) = \left| \int d^3X \, \mathrm{e}^{i\mathbf{p}_m \cdot \mathbf{X}} \chi_0(\mathbf{X}) \overline{\Omega}_{\mathbf{p}}^{(-)}(\mathbf{X}) \right|^2 . \tag{31}$$

The results discussed in the present paper have been obtained using the overlap $\chi_0(\mathbf{X})$ computed in ref.[16] using the Argonne v14 two-nucleon interaction and the Urbana VII three-body potential. The scattering operator $\overline{\Omega}_{\mathbf{p}}^{(-)}(\mathbf{X})$ has been calculated carrying out the integrations involved in eq.(19) with the Monte Carlo method, using a configuration set sampled from the probability distribution associated with the ^{4}He wave function of ref.[16].

In figs. 1 and 2 we show $W_{\mathbf{p}}(\mathbf{p}_m)$ evaluated at the top of the quasi free peak, i.e. at $\omega = Q^2/2m$, for parallel $(p_{m,\perp} = |\mathbf{p}_m \times \mathbf{q}| = 0)$ and perpendicular $(p_{m,z} = |\mathbf{p}_m \cdot \mathbf{q}| = 0)$ kinematics, respectively. Each figure has four panels, corresponding to different values of Q^2 ranging from 2 $(\mathrm{GeV/c})^2$ to 20 $(\mathrm{GeV/c})^2$. The dotted line shows the PWIA (i.e. $\overline{\Omega}_{\mathbf{p}}^{(-)}(\mathbf{X}) \equiv 1$) result, whereas the dashed and solid curves correspond to the calculations including FSI effects with and without CT, respectively. The configuration set employed in our calculations allows for an accurate determination of the missing momentum distribution over a large momentum range. However, in the region where $W_{\mathbf{p}}$ becomes very small $(\leq 10^{-4} \text{ fm}^3)$, the statistical uncertainty of the Monte Carlo calculation becomes sizeable. Although our results indicate that the first two-three excited states saturate the contribution of the off-diagonal rescatterings at missing momentum less than 300 MeV/c, we have included six intermediate states in all numerical calculations.

Fig. 1 shows that, while within PWIA $W_{\mathbf{p}}(p_{m,z}) = W_{\mathbf{p}}(-p_{m,z})$, FSI produce a forward bakward asymmetry, whose origin has to be ascribed to the effect of the real part of the NN scattering amplitude [20] and to the fact that the cancellation between the contributions of diagonal and off-diagonal rescattering processes depends upon the value of the missing momentum [21].

The main features of the distorted missing momentum distribution are the quenching in the region of the maximum, corresponding to $p_{m,z} \sim 0$, and the

enhancement of the tail at negative $p_{m,z}$. As expected, inclusion of CT reduces the effect of FSI.

A more complicated structure is observed in the case of perpendicular kinematics, shown in fig.2. The mimimum displayed by the PWIA missing momentum distribution, almost completely washed out by FSI, reappears at lower values of $p_{m,\perp}$ when the effect of CT is included. Note that at large $p_{m,\perp}$ ($p_{m,\perp} \geq 2$ fm$^{-}1$) the momentum distribution is dominated by FSI and that the inclusion of CT results in a sizable suppression.

The complex pattern of quenching and enhancement of the PWIA $W_{\mathbf{p}}$ has to be ascribed to the combined effects of FSI and strong NN correlations in the initial state. A similar behavior has been found in ref.[20], where the semi-inclusive process $^4He(e,e'p)X$ has been analyzed using the somewhat simplified Jastrow model to describe NN correlations. More recently, the $^4He(e,e'p)X$ reaction has been studied using a four-body wave function including noncentral correlations induced by the tensor component of the NN interaction [22]. The distorted momentum distributions of refs.[20] and [22] exhibit the same pattern of FSI effects on the S-wave contribution, while the D-wave is only weakly distorted. The main difference between the two approaches cancellation between the effects of central and tensor correlations at large missing momenta, leading to a suppression of the distortion by a factor of ~ 2.

The mimimum displayed by the PWIA missing momentum distribution, almost completely washed out by FSI, reappears at lower values of $p_{m,\perp}$ when the effect of CT is included. Figs. 1 and 2 show that at $Q^2 = 2$ (GeV/c)^2 and in absence of CT the missing momentum distribution at $p_{m,\perp} = p_{m,z} = 0$ gets quenched by 18 % on account of FSI.

The effects of FSI can be best observed in the ratio

$$T_p(\mathbf{p}_m) = \frac{W_{\mathbf{p}}(\mathbf{p}_m)}{|\int d^3X \mathrm{e}^{i\mathbf{p}_m \cdot \mathbf{X}} \chi_0(\mathbf{X})|^2} \ , \tag{32}$$

shown in figs. 3 and 4. It clearly follows from the definition that within PWIA $T_p(\mathbf{p}_m) \equiv 1$. When FSI are included, $T_p(\mathbf{p}_m)$ is a function of the missing momentum and can take values both above and below than unity, reflecting the fact that the distorted missing momentum distribution can be larger or smaller than the PWIA momentum distribution. Hence, in spite of the analogy between eq.(32) and the definition of the nuclear transparency, the quantity 1 - $T_p(\mathbf{p}_m)$ cannot be simply interpreted as the nuclear absorption experienced by a proton carrying momentum $\mathbf{p}$.

The calculated T_p corresponding to parallel and perpendicular kinematics are presented in figs. 3 and 4, respectively. The dotted curve shows the results obtained when no off-daigonal rescatterings are included, i.e. in absence of CT. The solid, dashed and long-dashed curves correspond to calculations in which CT effects have been taken into account by properly including off-diagonal rescatterings and using three different sets of parameters (α_1, α_2) to describe the real part of the scattering amplitudes associated with diagonal $(\alpha + N \rightarrow \alpha + N$, with $\alpha \neq p)$ and off-diagonal $(\alpha + N \rightarrow \beta + N$, with $\alpha \neq \beta)$ processes. These amplitudes have been parametrized according to:

$$Re \ f(\alpha + N \rightarrow \alpha + N) = \alpha_1 Re \ f(p + N \rightarrow p + N)$$
$$= \frac{\alpha_1}{3} \left[\alpha_{pp}\sigma_{pp} + 2\alpha_{pn}\sigma_{pn} \right] \ , \tag{33}$$

and

$$Re \ f(\alpha + N \rightarrow \beta + N) = \alpha_2 \ Im \ f(\alpha + N \rightarrow \beta + N) \ . \tag{34}$$

The results of our calculations turn out to be insensitive to the value of α_1, so we set $\alpha_1 = 1$ and show the effect of varying α_2 only. The solid, dashed and long dashed curves of Fig. 3 correspond to the sets $(\alpha_1, \alpha_2) = (1,0),(1,0.5)$ and $(1,-0.5)$. In parallel kinematics the dependence upon α_2 appears to be sizable, particularly at the largest value of Q^2. On the other hand, Fig. 4 shows that in perpendicular kinematics, where the effect of CT at large missing momentum is large, the theoretical error bar associated with the uncertainty in α_2 is rather small.

In fig. 5, we present the longitudinal forward-backward asymmetry of the missing momentum distribution defined as

$$A_z(x, y) = \frac{N_+ - N_-}{N_+ + N_-} \ , \tag{35}$$

where

$$N_\pm = \int_{\pm x}^{\pm y} dp_{m_z} \ W_{\mathbf{p}} \left(p_{m_z}, p_\perp = 0 \right) \ . \tag{36}$$

We have evaluated A_z from the above equations for four kinematical windows: $(x, y) = (0,0.3), (0,0.4), (0.05,0.3)$ and $(0.1,0.4)$ GeV/c. To illustrate the contribution of the off-diagonal rescattering processes to A_z, the results obtained setting these contributions to zero are shown by the dotted line. As in fig. 3 and 4, the solid, dashed and long-dashed lines correspond to different choices

of the parameter α_2. The results of fig. 5 show that even at moderate $Q^2 \sim 2.5$ $(\text{GeV/c})^2$, i.e. in the region relevant to the $(e, e'p)$ experimental program at the Thomas Jefferson National Accelerator Facility (TJNAF), off-diagonal rescatterings are responsible for more than 60 % of the calculated asymmetry for all of considered kinematical windows. In a previous study of the asymmetry in semi-inclusive $(e, e'p)$ processes we have found a contribution of 15-20 % and 10-15 % in the case of ^{16}O and ^{40}Ca, respectively [9]. The results of the present calculation confirm our conclusion that CT effects are larger in light nuclei. At $Q^2 le 20$ $(\text{GeV/c})^2$, our calculations show a weak dependence of A_z upon the value of the parameter α_2. Hence, the uncertainty associated with the chioce of α_2 does not prevent one from extracting an unambiguous signature of the onset of CT from the asymmetry.

4   Summary and conclusions

We have carried out a calculation of the missing momentum distribution of the process $^4\text{He}(e, e'p)^3\text{H}$ in quasielastic kinematics, i.e. at $\omega \sim Q^2/2m$, in the range $2 \le Q^2 \le 20$ $(\text{GeV/c})^2$.

The PWIA momentum distribution, evaluated using highly realistic manybody wave functions and the Monte Carlo method, has been corrected to include the effects of FSI, treated within a coupled-channel multiple scattering approach suitable to describe the possible onset of CT. It has to be emphasized that our approach allows for a consistent treatment of short range NN correlations in both the initial and final state.

Inclusion of FSI leads to the appearance of a complex pattern of distorsions of the PWIA momentum distribution, both in parallel and perpendicular kinematics. Sizable CT effects are observed in perpendicular kinematics at $p_{m\perp} \sim 1.5$ fm^{-1} over the whole Q^2 range. The CT signal turns out to be much larger than the theoretical uncertainty associated with the parametrization of the amplitudes for off-diagonal rescattering. The calculated forward-backward asymmetry also shows a significant CT effect already at $Q^2 \sim 2.5$ $(\text{GeV/c})^2$.

In conclusion, our results seem to indicate that the experimental study of the exclusive channels in $(e, e'p)$ processes off few-nucleon system may give a clue to the issue of the possible manifestation of CT in the domain of moderate Q^2 (≤ 3 $(\text{GeV/c})^2$), covered by the existing electron scattering facilities.

Acknowledgements

References

[1] *Modern Topics in Electron Scattering*, edited by B. Frois and I. Sick (World Scientific, Singapore, 1991).

[2] T. De Forest, Jr., Nucl. Phys. **A392** (1983) 232.

[3] S. Boffi, C, Giusti and F.D. Pacati, Phys. Rep. **226** (1993) 1.

[4] P.K.A. De Witt Huberts, J. Phys. G **16** (1990) 507.

[5] O. Benhar, A. Fabrocini, S. Fantoni, V.R. Pandharipande, S.C. Pieper and I. Sick, Phys. Lett. **B 359** (1995) 8.

[6] V.R. Pandharipande and S.C. Pieper, Phys. Rev. C **45** (1992) 791.

[7] S.J. Brodsky, in *Proceedings of the Thirteenth International Symposium on Multiparticle Dynamics*, edited by E.W. Kittel, W. Metzger and A. Stergion (World Scientific, Singapore, 1982).

[8] A. Mueller, in *Proceedings of the Seventh Rencontre de Moriond*, edited by J.Tran Thanh Van (Editions Frontieres, Gif-sur-Yvette, 1982).

[9] O. Benhar, S. Fantoni, N.N. Nikolaev, J. Speth, A.A. Usmani and B.G. Zakharov, Phys. Lett. **B 358** (1995) 191.

[10] O. Benhar, S. Fantoni, N.N. Nikolaev, J. Speth, A.A. Usmani and B.G. Zakharov, JETP **83** (1996) 1063.

[11] O. Benhar, S. Fantoni, N.N. Nikolaev, J. Speth, A.A. Usmani and B.G. Zakharov, Z. Phys. A **355** (1996) 191.

[12] R.J. Glauber, in *Lectures in Theoretical Physics*, edited by W.E. Brittin *et al* (Interscience Publishers Inc., New York, 1959).

[13] M.L. Goldberger and K.M. Watson, *Collision Theory* (J. Wiley & sons, New York, 1964).

[14] O. Benhar, in *Electron nucleus scattering*, edited by O. Benhar and A. Fabrocini, (ETS, Pisa, 1997).

[15] M. Radici, S. Boffi, S.C. Pieper and V.R. Pandharipande, Phys. Rev. C **50** (1994) 3010.

[16] R. Schiavilla, V.R. Pandharipande and R.B. Wiringa, Nucl. Phys. **A 449** (1986) 219.

[17] A.V. Dobrovolski *et al*, Nucl. Phys. **B214** (1983) 757.
B.H. Silverman *el al*, Nucl. Phys. **A499** (1989) 763.
W. Grein, Nucl. Phys. **B131** (1977) 255.

[18] N.N. Nikolaev, A. Szczurek, J. Speth, J. Wambach, B.G. Zakharov and V.R. Zoller, Nucl. Phys. **A567** (1994) 781.

[19] A. Bianconi, S. Jeschonnek, N.N. Nikolaev and B.G. Zakharov, Phys. Lett. **B338** (1994) 123.

[20] A. Bianconi, S. Jeschonnek, N.N. Nikolaev and B.G. Zakharov, Nucl. Phys. **A608** (1996) 437.

[21] N.N. Nikolaev, A. Szczurek, J. Speth, J. Wambach, B.G. Zakharov and V.R. Zoller, Phys. Lett. **B317** (1993) 281.

[22] C. Ciofi degli Atti, and D.Treleani, Phys. Rev. C **60** (1999) 034603.

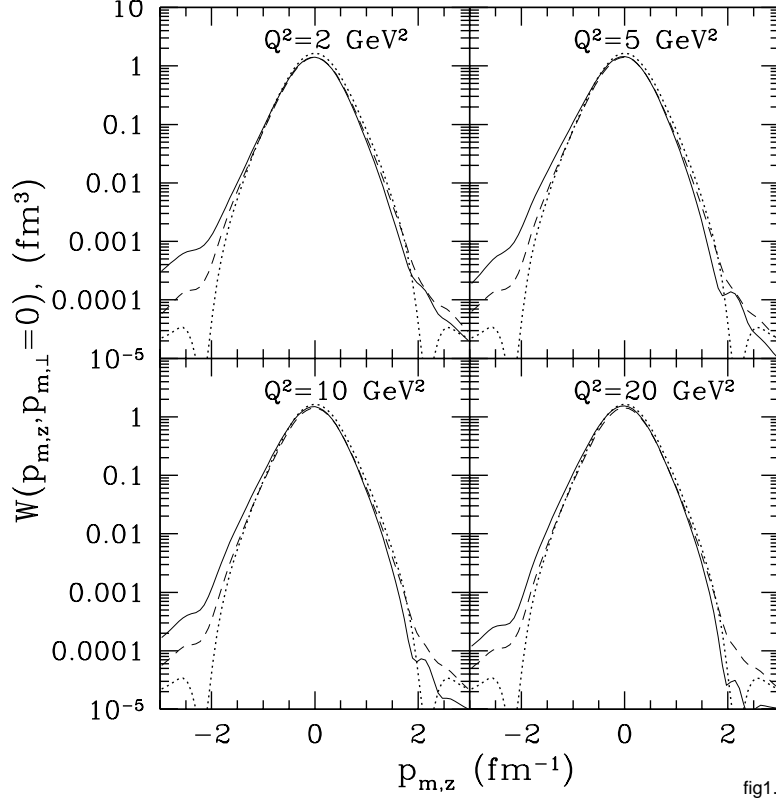Fig. 1. Missing momentum distribution for the process $^4He(e,e'p)^3H$, evaluated at the top of the quasifree peak in parallel kinematics. The dotted line shows the PWIA result, whereas the dashed and solid curves correspond to the calculations including FSI effects with and without color transparency, respectively.
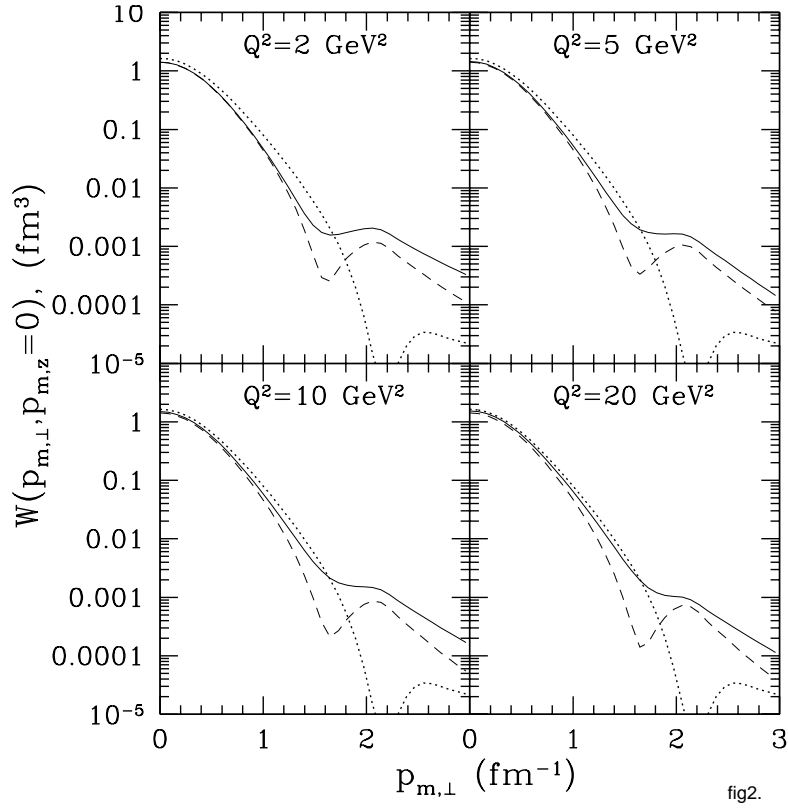
Fig. 2. Missing momentum distribution for the process $^4He(e,e'p)^3H$, evaluated at the top of the quasifree peak in perpendicular kinematics. The dotted line shows the PWIA result, whereas the dashed and solid curves correspond to the calculations including FSI effects with and without color transparency, respectively.
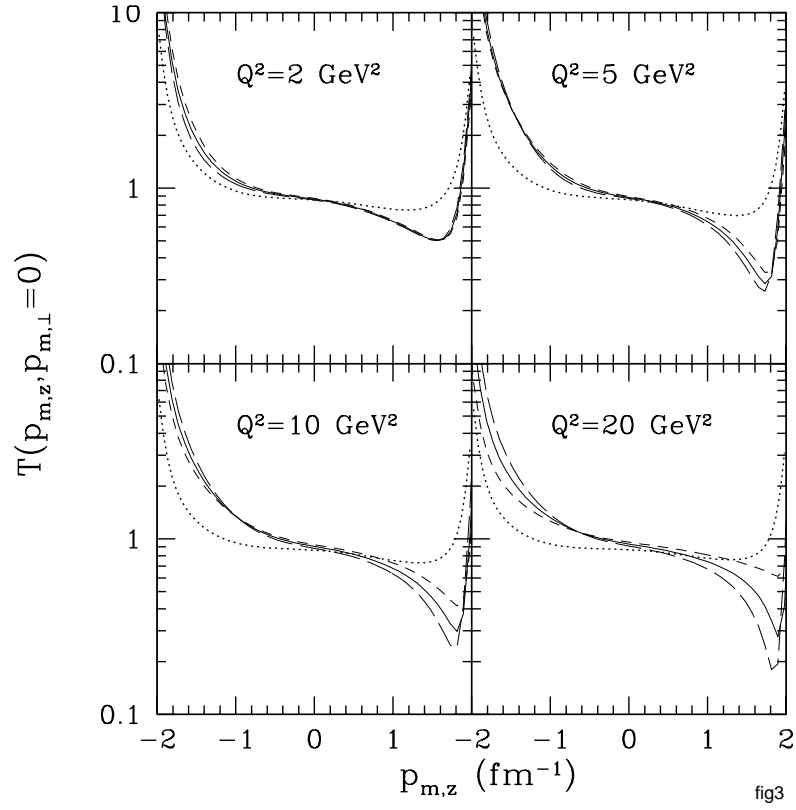
Fig. 3. Transparency ratios defined by eq.(32) and corresponding to the missing momentum distributions of fig.1.
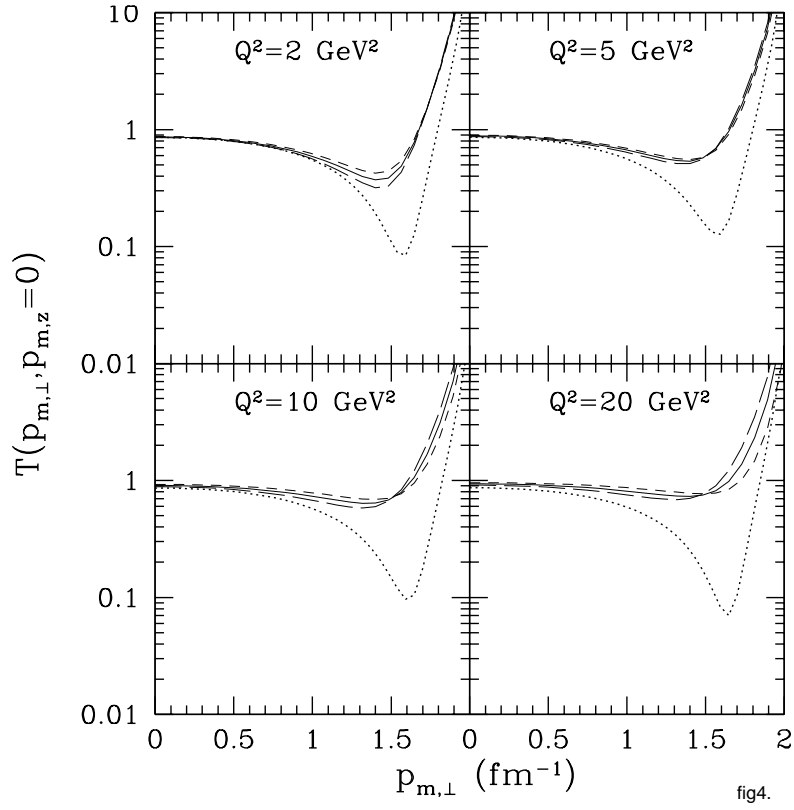
Fig. 4. Transparency ratios defined by eq.(32) and corresponding to the missing momentum distributions of fig.2.
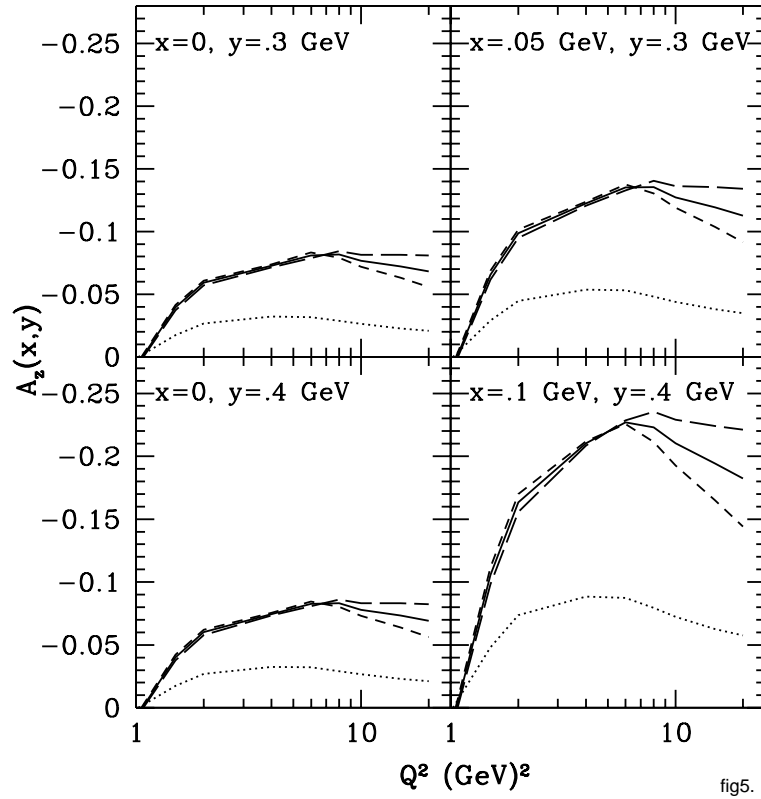
Fig. 5. Q^2 dependence of the longitudinal forward-backward asymmetry, defined as in eqs.(35)-(36), corresponding to four different kinematical windows.